ILASS 2008
Sep. 8-10, 2008, Como Lake, Italy

Paper ID ILASS08-5-4

A MODEL FOR THE CHARGE DENSITY PROFILE IN THE ORIFICE CHANNEL OF A CHARGE INJECTION ATOMIZER

John Shrimpton

Energy Technology Research Group
School of Engineering Sciences
University of Southampton
Southampton S017 1BJ
UK

ABSTRACT

Injection of electric charge into a dielectric and electrically insulating liquid produces a volume charge density distribution. In a charge injection atomizer some of this volume charge is convected out of the atomizer and the electric charge contributes to the destabilization of the liquid jet, leading to enhanced primary atomization and spray dispersion. Experimental studies show that the maximum charge density the liquid jet may contain is limited by a corona discharge surrounding the liquid jet as it emerges from the atomizer, suggesting the air surrounding the jet breaks down due to the electric field strength on the surface of the jet being exceeded. It is also observed that there exists a weak Reynolds number (based on the orifice channel flow) dependence of the maximum charge density. Assuming the charge density profile is uniform across the orifice radius a simple analytical solution shows a sensible estimate of the surface electric field strength, but an absence of Reynolds number dependence. Here a model of the radial charge density profile is developed that is non-uniform, and subject to boundary conditions that derive from experimental measurements.

INTRODUCTION

Electrostatic atomization is the addition of electric charges to the liquid jet which introduces disruptive electrical forces, breaking the jet into fine droplets. This method of electrostatic atomization has numerous advantages with respect to the quality of atomization such as small droplets and a narrow droplet size range, self dispersion of the spray and better control of the droplet size distribution [1-2]. For electrically semi-conducting liquids such is methanol, ethanol, doped heptane, and aqueous solutions several methods of generating electrically charged spray plumes are available, and some of these have been adopted for industrial use [3-8].

The electrostatic atomization of highly electrically insulating hydrocarbon fuels has been studied extensively in the past several decades. The application of this method started from the work of Kim and Turnbull [9], although research of charge-injection into liquid dielectrics was probably initiated by Tobazeon [10] in 1966. Kim and Turnbull used a needle with a chemically etched tip of radius less than 1μm placed inside a glass capillary, and grounded plate electrode at some distance. However, low flow rates and currents limited the usefulness of their atomizer. Kelly [11-12] greatly advanced the concept by developing the “spray triode” and solved the low flow rate/current problem by placing a grounded orifice near the emitter electrode. This is similar in concept to a device proposed by Jido [13].

The electrostatic charge-injection atomizer has been evolved over the past three decades [11-15]. Increasing the spray specific charge and reducing the leakage charge to atomizer ground is always desirable for improving spray quality. Several atomizer nozzles were tested and optimized extensively in the past years to understand the dependence on spray specific charge as a function of nozzle geometry, electrode position from grounded surface, orifice diameter and liquid viscosity. Publications arising from the research effort may be grouped according to understanding and optimizing the atomizer in terms of geometry, operating conditions and liquid fluid properties [16-21], properties of the charged drops and the charged spray plume [22-27] and prediction of inertial charged spray dynamics [28-29]. The work published [13-27] uses a simple ‘point-plane’ atomizer concept (Fig. 1) where the ‘point’ is a negative high voltage electrode emitting a total current I_T .

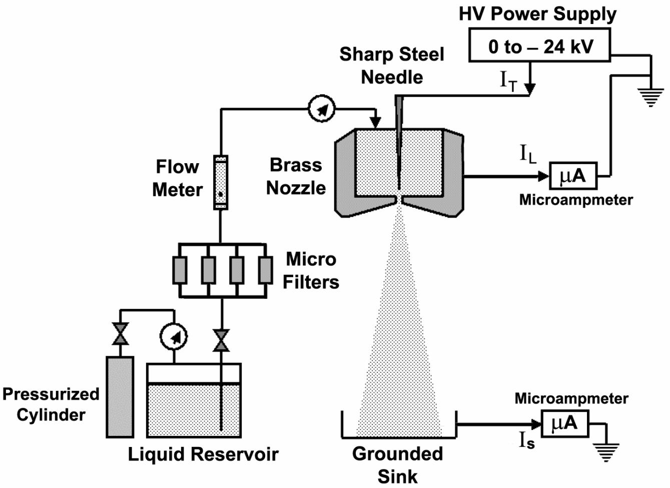

Figure 1 : The point-plane charge injection atomizer concept showing spray, leakage and total current paths

Some of this current is convected out of the atomizer, forming the spray current, I_S , and the remainder passes across the electrically insulating liquid and to earth through the atomizer body, and is termed the leakage current, I_L. The quotient of the spray current and the volume flow rate, $\dot{\tau}$ defines the mean spray specific charge $\overline{Q}$.

As discussed elsewhere [22,23,27] the spray quality improves when the mean injection velocity, $\overline{U}$ and the mean spray specific charge, $\overline{Q}$ increase, with the former variable having a minor effect over the mean velocity range currently analysed ($\overline{U}_{\max}$~30m/s). The process that limits the maximum spray specific charge a spray may contain has been shown photographically [18] to be due to a corona discharge at the orifice exit. Furthermore, correlating the operating conditions for a given liquid insulator, a correlation is found [18] where the orifice diameter and the spray specific charge obey approximately the relation,

$$\overline{Q}R \sim const + f(\mathrm{Re}) \qquad (1)$$

and that the constant of eq (1) is approximately 3e6 V/m, the electrical breakdown strength for air at atmospheric pressure [30].

This may be compared to an analytical relationship between the spray specific charge and the orifice radius and the limiting electric field at the wall, E_R [18] assuming the following :

1. Uniform velocity for all r
2. Uniform space charge for all r
3. $dV/dr\big|_{r=0} = 0$

$$E_R = \frac{\overline{Q}R}{4\varepsilon} \qquad (2)$$

where ε the electrical permittivity of the liquid insulator.

Comparing eqns. (1) and (2) shows that the experimentally observed flow influence is lost, and that therefore the ability for the mean flow speed and /or the velocity have an effect on the mean spray specific charge carried by the spray. This must be due to a non-uniform charge density and/or non-uniform velocity profile across the orifice. Further evidence of the effect of the velocity profile effect is suggested by experimental data of Kelly [31] using a charge injection atomizer of a design different from that of the point-plane concept. Here, the data suggests

$$\overline{Q}R^{1.8} \sim const \qquad (3)$$

with E_R~*15e6* V/m and no dependence on Reynolds number.

Two previous attempts are published which attempt to account for the effect of the radial profile of specific charge in the liquid jet on the overall mean spray charge density and thereby link geometry and operational characteristics of the atomizer and the liquid properties to the measured mean spray charge density [31-32]. Of the two the latter [32] is the more advanced and assumes a charge density profile of the form.

$$Q = Q_0 + br^e - cr^f \qquad (4)$$

where Q_0 is the charge density at the axis (r=0) and b,c,e,f are constants to be determined. Kelly [32] assumed a parabolic velocity profile, but only applied two constraints. The results of this model [32] showed that more charge density was concentrated towards the orifice wall, and this effect became more pronounced as the orifice radius increased from $r \sim 50\mu m$ to $r \sim 500\mu m$. This it has been claimed is the reason for a two-zone spray structure [33], where a sheath of small highly charged drops surrounds and core of larger less charged drops. This is possible, however it is not obvious from the model development of the charge density profile currently available [31-32] since eqn. (4) violates basic constraint in that $dQ/dr\big|_{r=0} \neq 0$. This, the discrepancy between empirical eqns. (1) and (3) and also the value of E_R motivated the derivation of a mathematically consistent model. This is now outlined.

MODEL DETAILS

The present model assumes constant conditions along the length of the cylindrical orifice channel of a charge injection atomizer. The velocity profile is assumed to be laminar as in [32],

$$U = U_0\left(1 - \left[\frac{r}{R}\right]^2\right) \qquad (5)$$

Where U_0 is the centreline velocity and $U_0 = 2\overline{U}$. The charge density profile is assumed to be represented by a 3rd order polynomial,

$$Q = a_0 + a_1 r + a_2 r^2 + a_3 r^3 \qquad (6)$$

Therefore, the problem becomes defining 4 constraints to define the 4 constants a_x of eqn. (6). The constants themselves are defined in appendix 1.

Constraint #1 : Zero Q gradient on the centreline.

The mathematical requirement $dQ/dr\big|_{r=0} = 0$ gives in eqn. (6),

$$a_1 = 0 \qquad (7)$$

This was absent from Kelly [32] and was possible only if *b=c=0* in eqn (4), which would have recovered the trivial solution eqn. (2).

Constraint #2 : Wall electric field equal to E_R.

This arises from integrating

$$\frac{1}{r}\frac{d}{dr}\left(r\frac{dV}{dr}\right) = -\frac{Q}{\varepsilon} \qquad (8)$$

and applying the boundary condition $-dV/dr\big|_{r=R} = E_R$. This was present in the model of Kelly [32]. This stems from the observation of corona discharge around the liquid jet as it emerges from the atomizer [18]. The value of E_R has yet to be determined.

Constraint #3 : Conservation of charge.

The bulk mean specific charge may be defined,

$$\overline{Q} = \frac{\int_0^R QUrdr}{\int_0^R Urdr} \qquad (9)$$

This was present in the model of Kelly [32].

Constraint #4 : Charge flux through the orifice wall.

This is obtained by defining the charge flux at the orifice wall to be due to the diffusion of charge at the wall,

$$J_Q = -\rho D \left.\frac{dQ}{dr}\right|_{r=R} \qquad (10)$$

where D is the molecular diffusion coefficient of the ions and ρ is the liquid density. The flux J_Q is known from experimental measurements of the leakage current and the area of the orifice channel at r=R, therefore,

$$\left.\frac{dQ}{dr}\right|_{r=R} = -\frac{2\pi RLI_L}{D} = C \qquad (11)$$

Where L is the length of the orifice channel and C is a constant used in appendix 1. This was absent from Kelly [32].

MODEL CONSTRAINT DATA

In the present study, data for the fluid properties and the operating conditions and geometry of the atomizer are obtained from previous work and the data required for the model testing is listed in table 1. Cases 1 to 13 are data obtained by the author directly [14], cases 14 to 17 from Rigit, at the time under the supervision of the author [15], cases 18 to 26 from the work of Balachandran et al [34] and cases 27 to 29 from the work of Nikitopoulos and Kelly [35] and Bankston et al [36]. More data in the literature is available authored or co-authored by Kelly, but none if it with the exception of [35] and [36] contains more than 3 of the parameters required. Of the data gathered, all information is available for cases 1 to 26 [14-15,34]. For cases 27 to 29 [35-36], the problem is the leakage current information. Kelly [37] states that the leakage current, as a fraction of the total current ranges from ~1% for liquids of conductivity ~10^{-12} $(\Omega\text{m})^{-1}$ to ~90% for liquids of conductivity ~10^{-10} $(\Omega\text{m})^{-1}$ [37]. There is one reference where a precise value of leakage current may be calculated, reference [36]. Here, Fig. 7 of this reference states that $\dot{\tau}$ =0.33cm^3/s through an orifice of 422μm. This is correct, since it gives a mean injection velocity of ~2.4m/s, which agrees with what is given in the paper. The total current is also available since the voltage and the total power consumption (10kV and 2.5mW respectively are given) give I_T =0.25μA. The spray current is also available from the same reference, since the flow rate and the spray charge density are available ($\dot{\tau}$ =0.33cm^3/s and $\overline{Q}$ =1.5C/m^3 respectively) giving I_S =0.50μA. Clearly, since $I_S > I_T$ the data provided in [36] has an error, and here it is assumed for cases 27 to 29 the leakage current is 5% of the spray current. The operating conditions with which to test the model encompass a reasonably wide range and are given as follows :

	R μm	Liquid (table2)	$\overline{Q}$ C/m^3	I_L μA	$\dot{\tau}$ ml/min	$\overline{U}$ m/s
1	500	K	0.08	0.5	75	1.59
2	250	K	0.57	1.0	75	6.36
3	250	D	0.65	1.1	120	10.1
4	250	D	0.68	1.8	150	12.7
5	250	D	0.65	0.5	214	18.6
6	250	K	0.70	1.2	120	10.1
7	*125*	K	1.40	2.0	30	10.1
8	75	K	1.64	1.0	11	10.1
9	75	K	2.40	0.9	20	18.6
10	75	K	3.00	0.8	30	28.3
11	75	K	2.85	0.7	40	37.7
12	150	K	1.07	1.0	45	10.6
13	250	K	0.63	1.2	120	10.18
14	58	D	4.40	11	15.6	10.18
15	58	D	4.00	2.1	9.3	24.6
16	58	D	2.75	0.7	6.3	14.6
17	58	D	2.40	0.3	4.2	9.9
18	315	K	0.20	0.7	100	6.6
19	315	K	0.26	1.5	175	5.3
20	315	K	0.36	2.7	225	9.3
21	500	K	0.19	0.6	100	12.0
22	500	K	0.22	1.3	175	2.12
23	500	K	0.23	1.7	225	3.71
24	750	K	0.05	0.2	100	4.7
25	750	K	0.06	0.3	175	0.9
26	750	K	0.07	0.5	225	1.6
27	500	M	0.15	0.038	300	6.36
28	86.5	D	1.5	0.045	36	25.5
29	211	O	1.5	0.025	20.1	2.4

Table 1 : Operating conditions

For all of these cases L of eqn (11) is equal to $2d$. Liquid physical properties are listed in table 2. 'kerosene' (K), an aviation like fuel and standard UK Diesel oil (D), are circa mid 1990's. The marcol-87 (M) and mineral oil (O) liquids have physical properties listed in references [35] and [36]. The molecular diffusivity is estimated using the Stokes-Einstein relation,

$$D = \frac{k_B T}{q}\kappa \qquad (12)$$

Where k_B is the Boltzmann constant, T the temperature, κ the ion mobility and q the electron charge. The ion mobility may be related to the liquid viscosity [1] giving

$$D \approx \frac{3e^{-10}}{\mu} \qquad (13)$$

Liquid	Kerosene (K)	Diesel oil (D)	Marcol-87 (M)	Mineral oil (O)
ε	2.2	2.2		
μ	0.0011	0.0023	0.0035	0.0025
D	2.7e-7	1.3e-7	0.85e-7	1.2e-7

Table 2 : Physical Properties

MODEL PERFORMANCE

Figure 2 shows the output from the model for all of the cases shown defined in table 1, for E_R~3e6V/m, where the y axis is the actual charge density plotted as a function of the non-dimensional radial displacement. With one important exception, addressed below, all of the Q points, for all cases are positive. Given that the charge cannot change sign, and the fact that there is no explicit restriction within the model for this condition considering we are fitting a reasonably flexible polynomial over a very wide range as detailed in table 1 gives some confidence that the method is consistent.

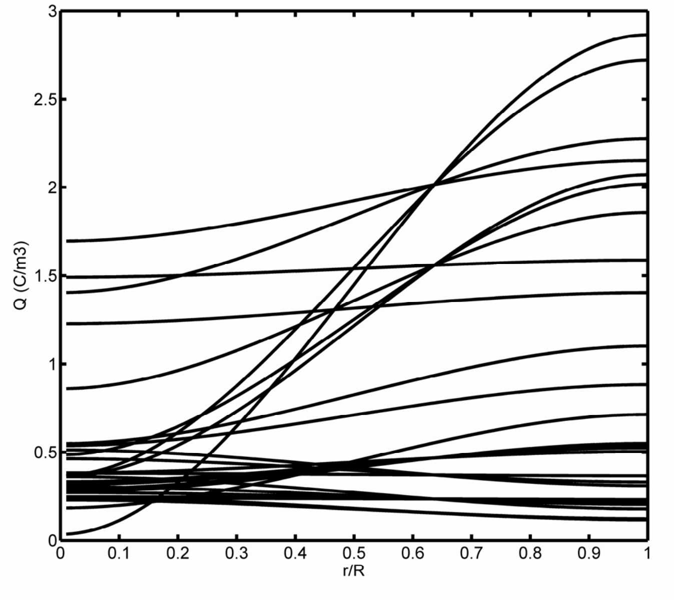

Figure 2 : Charge density profiles versus non-dimensional radius for all cases listed in table 1.

This first glance shows that there are deviations from the analytical solution assuming uniform radial charge density (eqn 2) with both the inner and the outer regions of the liquid columns possessing peak values. It should be noted that all charge density profiles sum to the bulk mean defined in table 1, by virtue of constraint #3, and also the wall electric field is the breakdown strength for all cases. The electric field radial profiles for all cases are given in Fig. 3, and show a non-linear variation about the linear relation arising from the analytical solution of eqn (2).

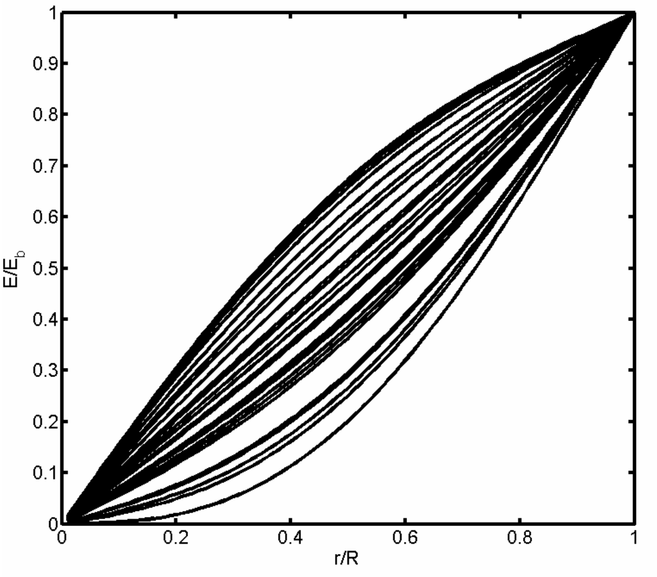

Figure 3 : Non-dimensional electric field profiles versus non-dimensional radius for all cases listed in table 1.

The one test listed in table 1 that required modification to ensure Q>0 for all r was test 29, and it is noted that this is the only test where the spray current exceeds the total current by a factor of ~2. It was found that reducing $\overline{Q}$ from 1.5 to 1C/m^3 gives a realizable result. This issue is illustrated with this case and a similar data-set from [14] to show that the consistency demonstrated in Figure 2 is a product of the fact that the data values for the variables in each case are internally consistent and the model will produce non-realizable predictions with non-realizable input sets. Figure 4 shows 5 sets of data, 3 arising from case 2, changing the value of $\overline{Q}$, and two sets of data from case 29, one of which is the value given in table 2 ($\overline{Q}$ =1.5C/m^3) and one the value used in Figure 2 ($\overline{Q}$ =1C/m^3).

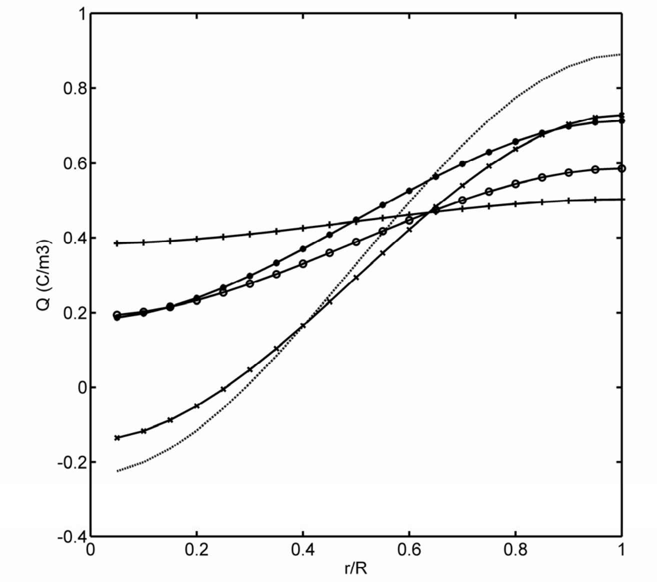

Figure 4 : Charge density profiles for case 2 of table 1 (+ : $\overline{Q}$ =0.57C/m^3, o : $\overline{Q}$ =0.8C/m^3, x : $\overline{Q}$ =1.2C/m^3) and case 29 (…: $\overline{Q}$ =1.5C/m^3, ● : $\overline{Q}$ =1.0C/m^3)

It is observed that in case 29 as the charge density is reduced from the published value ($\overline{Q}$ =1.5C/m^3) to the suggested value ($\overline{Q}$ =1.0C/m^3) the charge density profile becomes realizable. Similarly case 2 (a completely different atomizer design) can be observed produce a similar kind of behaviour here the charge density gradually becoming non-realizable as the charge density increases. The physical interpretation of this is that the there is too much charge density to apportion over the radial span in these problem cases whilst maintaining the electric field boundary condition (constraint #2). The mathematical solution is to define charge of the opposite sign to meet this criteria and place this near to the axis where it has less impact on the near wall electric field. It seems that the model proposed produces sensible output only provided the inputs are sensible. Given that there exists a 5 dimensional parameter space to define a set of inputs, and that the cases listed in table 1, with one exception as discussed, all produce sensible output. This gives some confidence that the model is well posed and reasonably reliable, to the extent that the model can indicate what constraint set is not viable. From a design point of view, this is extremely useful.

We now turn to investigating some of the characteristics of the predictions introduced briefly in Figure 2. Focussing on the large diameter and small orifice diameter datasets reveals the separation of the data in terms of where the peak in is terms of which side of r/R from Fig. 2. Figure 5 shows the data from cases 18-20 and 24-26, a range of conditions where the orifice diameter is relatively large, the spray charge densities relatively small (which can be understood via eqn 2) and a reasonable span of mean velocities. It is shown that the charge density profiles are predicted to be larger near the axis and flatten as the charge density increases. Conversely, Figure 6 shows the charge density profiles from cases 14 to 17, the conditions with the smallest orifice diameters and the largest mean spray charge. Here it is observed that the peak lies towards the wall, and increases with increase in charge density. Figure 7 shows the electric field profiles for these cases. The near axis electric field is suppressed by moving the charge away from the axis and towards the wall and this gives the explanation for what is being observed generally.

Given the constraints, the problem in words is how 'does one fit a given amount of space charge across a certain size orifice given that the velocity differential across the radius is prescribed and that the electric field at the edge is fixed'. The predictions given give the unique answer for each of the constraint sets. From a design point of view the question is : 'what is the maximum amount of space charge can one define for a given set of constraints'. The generic shape of the optimal profile can be inferred from the meaning behind Figs. 5 and 6, in that the best radial location to 'place' space charge for minimal impact on the electric field at the wall is near the wall. This suggests that from Fig. 6 that case 14 is very nearly at the maximum mean spray charge density attainable, any further increase would precipitate a negative near axis space charge, as has already been illustrated in Fig. 4. Conversely, the results from Fig. 5 suggest that the large diameter charge injection atomizer could be improved.

Comparing these results to the predictions of Kelly [32], the high charge/small orifice diameter shape of the radial charge density profile is similar, but only because this was the assumed shape proposed in the case of [32]. The low charge density/large orifice diameter shape change is not apparent in the earlier model [32], because it is not possible. The present approach applies more constraints and invokes very little empiricism. It gives sensible predictions for a wide range of constraint sets from data generated by several authors with 3 independent atomizer configurations.

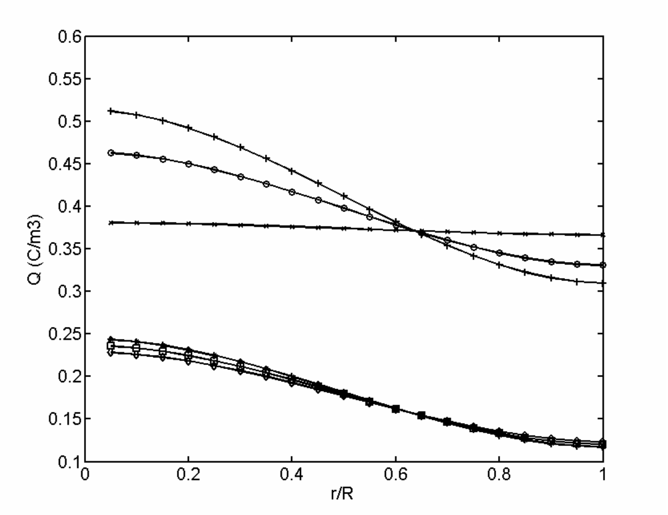

Figure 5 : Charge density profiles for the low mean spray charge and large orifice diameter case, cases 18 (+), 19 (o), 20 (x), 24 (*), 25 (□) and 26 (◊)

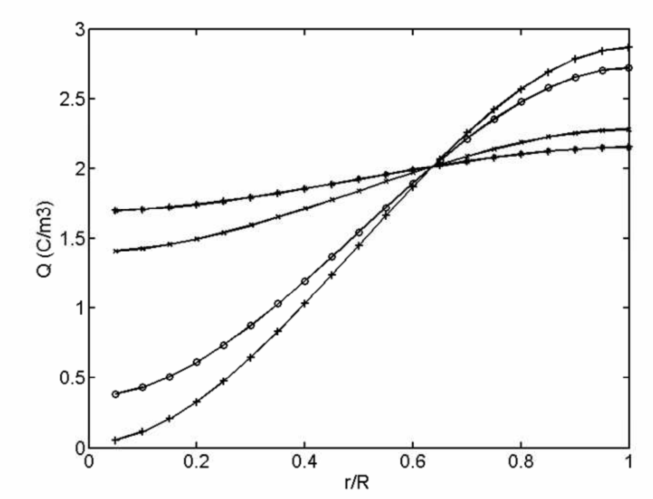

Figure 6 : Charge density profiles for the high mean spray charge and small orifice diameter case, cases 14 (+), 15 (o), 16 (x) and 17 (*)

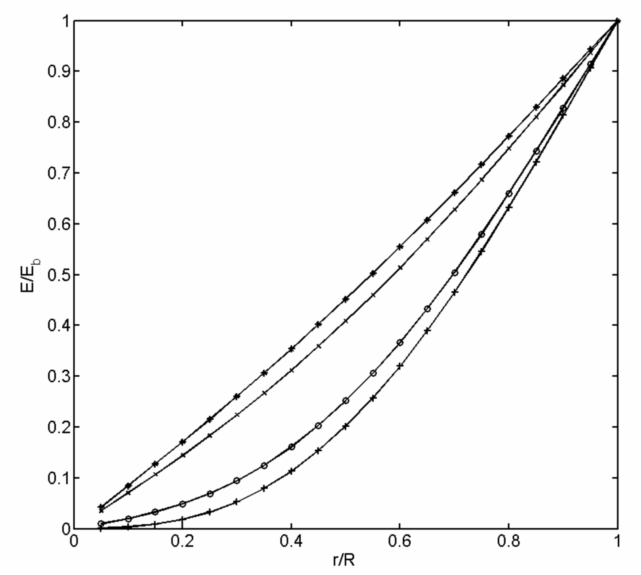

Figure 7 : Normalised electric field profiles for the high mean spray charge, cases 14 (+), 15 (o), 16 (x) and 17 (*)

CONCLUDING REMARKS

It should be remembered that the predictions derive from mathematical constraints placed upon a freely definable polynomial. The constraints are well posed, and providing the input data used to numerically quantify the polynomial constants are sensible, then the prediction should be similarly sensible. The choice of input data used here has used the widest possible range currently available in the literature. There exists a 5 dimensional parameter space and the 5 parameters vary by the following amounts

Orifice diameter : 1 order.
Mean spray specific charge : 2 orders.
Leakage current : 3 orders.
Injection velocity : 2 orders.
Diffusion Coefficient : 0 orders.

Within the constraints of the available data, the predictions, with one exception are realizable and sensible. The source of the one exception contains a verifiable error in the manuscript, and should not, in the authors view, detract from the remainder of this work.

Further work is required concerning investigating the effect of the diffusion coefficient, requiring more viscous liquids, and also the effect of variation of the velocity profile beyond the current laminar profile. Validation against CFD simulations of the internal nozzle flow would also be extremely useful.

Once this work is complete a useful design tool will be available to guide the design of charge injection atomizers. It will still need an understanding of electrohydrodynamics and empirical knowledge to design a charge injection atomizer to produce the optimised charge density profile, however now there is the possibility to probe the parameter space analytically, and to know what the desired charge density profile is.

NOMENCLATURE

Symbol	Quantity	SI Unit
$\overline{U}$	Bulk mean injection velocity	m/s
$\overline{Q}$	Bulk mean spray specific charge	C/m^3
I_T	Total current emitted from the high voltage electrode	A
I_S	Spray current	A
I_L	Leakage current	A
R	Radius of the atomizer orifice	m
E_R	Electric field at the orifice wall/jet surface	V/m
ε	Electrical permittivity of the liquid	F/m
Re	Reynolds number based on the orifice length and velocity scale	(-)
J_Q	Current flux at r=R	A/m^2
ρ	Liquid density	kg/m^3
μ	Dynamic viscosity	Ns/m^2
D	Diffusion coefficient for ions	m^2/s
$\dot{\tau}$	Volume flow rate	m^3/s

REFERENCES

[1] Crowley J. M. (1999), “Fundamentals of Applied Electrostatics”, 1st Ed., Laplacian Press, Morgan Hill, California

[2] J. S. Chang, J. M. Crowley, and A. J. Kelly, Handbook of Electrostatic Processes. Dekkar, 1995.

[3] Ye Q, Steigleder, Scheibe A, Domnick J (2002), Numerical simulation of the electrostatic powder coating process with a corona spray gun, Journal of Electrostatics, 54, 2, p. 189-205.

[4] Cloupeau M and Prunet-Foch B, 1990, "Electrostatic spraying of liquids : Main functioning modes", J. Electrostatics, 25, pp. 165-184.

[5] Law SE, 1978, "Embedded electrode electrostatic spraying charging nozzle", Trans. ASAE, pp. 1096-1104.

[6] Agui T and Nakajima M, 1977, "Drop formation characteristics of electrostatic ink jets using a water based ink. ", IEEE Trans. Electron Devices. ED24, 3, pp. 262-266.

[7] Griffiths, WJ, Jonsson, AP, Liu, S, Rai DK, Wang, Y, Electrospray and tandem mass spectrometry in biochemistry , Biochem. J. (2001) 355 (545–561)

[8] Kyritsis DC, Coriton B, Faure F, Roychoudhury S, Gomez A, Optimization of a catalytic combustor using electrosprayed liquid hydrocarbons for mesoscale power generation, Combustion and Flame 139 (2004) 77–89

[9] K. Kim, and R.J. Turnbull, Generation of Charged Drops of Insulating Liquids by Electrostatic Spraying, J. Appl. Physics, vol 47, pp. 1964-1969, 1976.

[10] R. Tobazeon, Ph.D. thesis, University of Grenoble, Grenoble, France, 1966.

[11] A.J. Kelly, The Electrostatic Atomization of Hydrocarbons, J. Inst. Energy, vol. 57, pp. 312–320, 1984.

[12] A.J. Kelly, Electrostatic Atomizing Device, United States Patent 4,255,777, March 10, 1981.

[13] M. Jido, Study of Electrostatic Charged Droplets: Part 1, J. Jpn. Soc. Chem. Eng., vol. 40, pp. 24-33, 1986.

[14] J. S. Shrimpton, Electrostatic Atomization and Combustion of Hydrocarbon Oils, Ph.D. thesis, University of Manchester Institute of Science and Technology, Manchester, UK, 1995.

[15] A. R. H. Rigit., Performance of a Charge-injection Electrostatic Atomizer and Spray Characteristics, Ph.D. thesis, Imperial College, London, UK, 2005.

[16] J.S. Shrimpton, AJ Yule, AP Watkins, W Balachandran and D Hu, Electrostatically atomized hydrocarbon sprays, Fuel J., Vol 74, pp.1094-1103, 1995.

[17] J.S. Shrimpton, D Hu, W Balachandran, A.J Yule and AP Watkins, Electrostatic atomization of insulating oils and the associated charge injection mechanism, Inst. Phys. Conf. Series, No.143, pp.205-210., 1996.

[18] J.S. Shrimpton, AJ Yule, 'Electrohydrodynamics of charge injection atomization : Regimes and fundamental limits', Atomization and Sprays, vol. 13, pp. 173-190, 2003.

[19] J.S. Shrimpton, AJ Yule, 'Design issues concerning charge injection atomizers', Atomization and Sprays, vol. 14, pp. 127-142, 2004

[20] J.S. Shrimpton, ARH Rigit, Electrical performance of charge injection atomizers, Atomization and Sprays, 16, 4, 2006,

[21] Al-Ahmad G., Shrimpton J.S., Ergene E. L., Mashayek F, 2008, Atomization of pure liquid organic oils using the charge injection method', submitted to Atomization and Sprays.

[22] J.S. Shrimpton, AJ Yule, Drop size and velocity measurements in an electrostatically produced hydrocarbon spray., Journal of Fluids Engineering, Transactions of ASME, Vol 120, no 3, Sept 1998, pp. 580-585.

[23] J.S. Shrimpton, AJ Yule, Characterisation of charged hydrocarbon sprays for application to combustion systems, Experiments in Fluids, 26, 4, 1999

[24] J.S. Shrimpton AJ Yule, Atomization, combustion and control of charged hydrocarbon sprays, Atomization and Sprays, 11, pp. 1-32, 2001

[25] J.S. Shrimpton, MCY Wong, Drop - Charge correlations for polydisperse electrostatically atomized liquid sprays, IEEE Trans. Dielectrics and Electrical Insulation, vol 11, no. 2, pp. 362-368, 2004.

[26] J.S. Shrimpton, Dielectric Charged Drop Break up at Sub-Rayleigh Limit Conditions, IEEE Trans. Dielectrics and Electrical Insulation,. Vol.12, n 3, pp.573-578, 2005

[27] J.S. Shrimpton, ARH Rigit, Spray characteristics of charge injection atomizers with small orifice diameters, Atomization and Sprays, 16, 4, 2006, p421-442

[28] Shrimpton JS 'Pulsed Charged Sprays : Application to DISI Engines during Early Injection', International Journal for Numerical Methods in Engineering, vol 58, pp. 523-536, 2003

[29] Shrimpton, JS and Y Laoonual, "Dynamics of Electrically-Charged transient evaporating sprays", International journal for numerical methods in engineering, 67, 8, p.1063-1081, 2006.

[30] Peek F W 1929 Dielectric Phenomena in High-Voltage Engineering, New York: McGraw-Hill.

[31] Kelly, A.J. Charge injection electrostatic atomizer modelling, Aerosol Science and Technology, 12, p. 526-527, 1999

[32] Kelly, A.J. Charge injection electrostatic performance modelling, ICLASS-88, August 22-24, 1988, Sendai, Japan.

[33] Kelly A.J. On the statistical, quantum and practical mechanics of electrostatic atomization, J. Aerosol Sci, 25, 6, p. 1159-1177, 1994.

[34] Balachandran, W., Machowski, W., Halimic, M., Morgan, L., Gray, C., and Wilson, C., "Development of an Electrostatic Nozzle for Gas Turbine Applications," Proc. ILASS, Toulouse, France, 1999.

[35] Nikitopoulos DE and Kelly, A.J. Formation of a Net Negative charged Liquid Spray, Physics of Fluids, 12, 9, Sept. 2000, S7.

[36] Bankston CP; Back LH; Kwack EY; Kelly AJ (1988). Experimental investigation of electrostatic dispersion and combustion of diesel fuel jets. J. Eng. Gas Turbine and Power 110: 361-368.

[37] Kelly A.J. The electrostatic atomization of hydrocarbons, Proc. ICLASS-82, 20-24th June 1982, Concourse hotel, Madison, WI, USA, 1982.

APPENDIX 1

$$a_0 = \frac{2\varepsilon E_R}{R} + \frac{6}{59}\left(\frac{35\overline{Q}}{2} + CR - \frac{35\varepsilon E_R}{R}\right) - \frac{2}{5}\left(\frac{CR}{3} - \frac{8}{59}\left(\frac{35\overline{Q}}{2} + CR - \frac{35\varepsilon E_R}{R}\right)\right)$$

$$a_2 = \frac{12}{59}\left(\frac{35\overline{Q}}{2R^2} + \frac{C}{R} - \frac{35\varepsilon E_R}{R^3}\right)$$

$$a_3 = \frac{C}{3R^2} - \frac{8}{59}\left(\frac{35\overline{Q}}{2R^3} + \frac{C}{R^2} - \frac{35\varepsilon E_R}{R^4}\right)$$